Microchimica Acta
https://doi.org/10.1007/s00604-019-3532-4

ORIGINAL PAPER

UV-assisted chemiresistors made with gold-modified ZnO nanorods to detect ozone gas at room temperature

Nirav Joshi [1,2] · Luís F. da Silva [3] · Flavio M. Shimizu [1,4] · Valmor R. Mastelaro [1] · Jean-Claude M'Peko [1] · Liwei Lin [2] · Osvaldo N. Oliveira Jr [1]

Received: 11 February 2019 / Accepted: 19 May 2019

Abstract

Two kinds of flexible ozone (O_3) sensors were obtained by placing pristine ZnO nanorods and gold-modified ZnO nanorods (NRs) on a bi-axially oriented poly(ethylene terephthalate) substrate. The chemiresistive sensor is operated at typically 1 V at room temperature under the UV-light illumination. The ZnO nanorods were prepared via a hydrothermal route and have a highly crystalline wurtzite structure, with diameters ranging between 70 and 300 nm and a length varying from 1 to 3 μm. The ZnO NRs were then coated with a ca. 10 nm gold layer whose presence was confirmed with microscopy analysis. This sensor is found to be superior to detect ozone at a room temperature. Typical figures of merit include (a) a sensor response of 108 at 30 ppb ozone for gold-modified ZnO NRs, and (b) a linear range that extends from 30 to 570 ppb. The sensor is stable, reproducible and selective for O_3 compared to other oxidizing and reducing gases. The enhanced performance induced by the modification of ZnO nanorods with thin layer of gold is attributed to the increased reaction kinetics compared to pristine ZnO NRs. The sensing mechanism is assumed to be based on the formation of a nano-Schottky type barrier junction at the interface between gold and ZnO.

Keywords Zinc oxide nanorods · Hydrothermal route · Ozone gas · Flexible sensor devices · UV-activation

Introduction

Room-temperature gas sensing is desirable to monitor and control gas emission associated with pollution and industrial processes [1, 2]. Power consumption during the sensor operation is also a concern for applications in battery-powered mobile healthcare systems and wearable sensing devices [3]. The challenge is to produce sensing units with these desirable features at a sufficiently low cost to allow for wide deployment, which can only be reached with efficient materials and fabrication procedures. Nanostructured metal oxides have been strong candidates for such sensors, especially in chemiresistor devices due to their wide bandgap. Zinc oxide (ZnO) is a multifunctional material with a wide band gap of 3.4 eV (at 300 K), excellent for gas sensing [4]. Pristine ZnO sensors have been reported to exhibit high sensitivity and fast response/recovery speed for detecting ammonia and ethanol with relatively high working temperatures which might limit sensor lifetime and stability [5]. On the other hand, sensing performance can be improved with UV-light activation [6] as a large number of photocarriers are generated when ZnO is illuminated by a UV-source. This can cause the decrease of both depletion layer width and the inter-grain barrier height to promote catalytic reactions between the target gases and oxygen ions [7, 8]. The precise mechanisms of this enhanced performance brought by UV illumination are still unclear, despite the successful use in metal oxide gas sensors [9].

Electronic supplementary material The online version of this article (https://doi.org/10.1007/s00604-019-3532-4) contains supplementary material, which is available to authorized users.

✉ Nirav Joshi
nirav.joshi1986@gmail.com

✉ Liwei Lin
lwlin@berkeley.edu

✉ Osvaldo N. Oliveira, Jr
chu@ifsc.usp.br

[1] São Carlos Institute of Physics, University of São Paulo, 369, São Carlos, São Paulo, CP 13560-970, Brazil

[2] Department of Mechanical Engineering, University of California, Berkeley, CA, USA

[3] Department of Physics, Federal University of São Carlos, Rodovia Washington Luis km 235, São Carlos, SP 13565-905, Brazil

[4] Brazilian Nanotechnology National Laboratory (LNNano), Brazilian Center for Research in Energy and Materials (CNPEM), Campinas, São Paulo 13083-970, Brazil

Published online: 11 June 2019

This manuscript describes the UV-assisted gas sensing properties of ZnO nanorods (NRs) and gold-modified ZnO NRs deposited onto flexible substrates. In order to probe the mechanisms responsible for the sensing, the structure, microstructure, and surface properties of the sensing units were investigated with X-ray diffraction (XRD), scanning electron microscopy (SEM), and X-ray photoelectron spectroscopy (XPS). Electrical measurements were employed to verify the enhanced sensor response with operation at room temperature induced by UV-irradiation, particularly when a gold layer was deposited onto the ZnO NRs. Also to be noted is that the sensors are produced on flexible substrates, in contrast to most sensing layers that are normally deposited on mechanically rigid substrates, such as alumina, glass, quartz or Si. This is in line with the trend toward flexible devices, e.g. solar cells, chemical sensors, supercapacitors, etc., with attracting features that include light weight, flexibility, transparency and low cost compared to their inorganic counterparts.

Experimental details

The chemical reagents zinc(II) acetate ($Zn(CH_3COO)_2{\cdot}2H_2O$ (99%)), cobalt(II) acetate ($Co(CH_3COO)_2{\cdot}4H_2O$ (99%)), sodium hydroxide (NaOH), hexamethylenetetramine (HMTA) and ethylene glycol ($HOCH_2CH_2OH$, A.R.) were supplied by Sigma-Aldrich Co. LLC. and used without any further purification.

Fabrication of the interdigitated flexible electrodes

Flexible interdigitated electrodes were fabricated via photolithography in a clean room by coating bi-axially oriented poly(ethylene terephthalate) (BOPET) sheets with interdigitated Pt electrodes with the linewidth and spacing of 50 μm, as shown in Fig. 1. The BOPET sheets were initially cleaned with deionized water and dried, according to Refs [10, 11], and then coated with a layer of positive photoresist AZ4210 using a spin coater (Chemat, KW-4A). An interdigitated pattern was created by exposing a photoresist film to UV light with a mask aligner (Karl Suss, MJB3) for 50 s. After developing the exposed area, 5 nm of chromium (adhesive layer) and 100 nm of Pt were deposited by sputtering (Leybold, Z400). The excess of photoresist was removed using a lift-off process. The substrate in Fig. 1 features an interdigitated Pt electrode with line width and spacing of 50 μm.

Hydrothermal growth of ZnO nanorods on flexible substrates

The ZnO nanorods were grown in-situ onto the flexible BOPET using the hydrothermal method [8], in which ZnO nanoparticles were first prepared by dissolving zinc acetate dihydrate

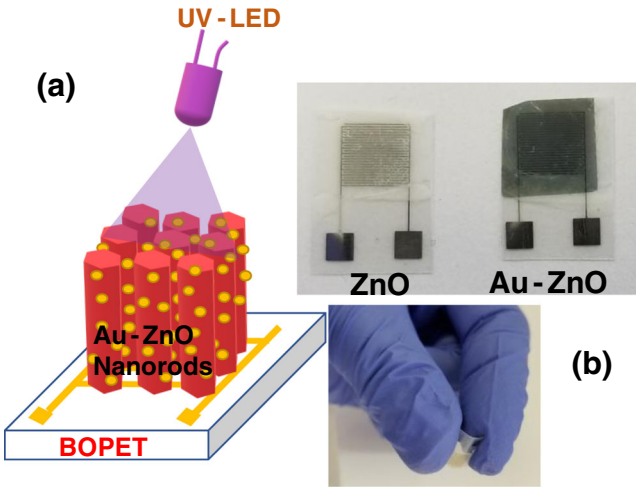

Fig. 1 Schematic illustration: (**a**) UV-enhanced flexible ZnO sensor; (**b**) Photos of flexible interdigitated electrodes fabricated with pristine ZnO and gold-ZnO

(30 mM) in methanol (250 mL) under stirring at 60 °C. Then, 15 mM of sodium hydroxide in methanol (250 mL) were added dropwise and the reaction mixture was stirred for 2 h at 60 °C. The ZnO seed solution was drop cast on the flexible interdigitated electrode and treated for 10 min at 60 °C. The growth of ZnO NRs on this flexible electrode occurred by suspending in an aqueous solution of zinc nitrate and HMTA at 95 °C for 7 h. The substrates were washed with deionized water and dried at 60 °C for 30 min. In the following step, the flexible substrates with the nanorods were functionalized with a 10 nm thick layer (i.e. a film, see the atomic force microscopy image in Fig. S1 in the Supporting Information) of gold by thermal evaporation under a vacuum pressure at 10^{-6} bar, current of 2.2 A applied during 21 s. A detailed description of gold deposition is given in [12, 13]. Henceforth, the gold modified ZnO films will be referred to as gold–ZnO. Figure 1 schematically illustrates the ZnO and gold-ZnO NRs deposited onto flexible substrates for the gas-sensing experiments.

Characterization and gas sensing measurements

The structural characterization of ZnO NRs was performed using X-ray diffraction (XRD) in a 2θ range from 30 to 60° with a 0.02° step at a 2° min^{-1} scanning speed using CuKα radiation (1.5406 Å; Rigaku, Rotaflex RU-200B). The microstructural analysis was carried out with field emission scanning electron microscopy (FE-SEM, Zeiss Sigma) operating at 5 kV, equipped with X-ray energy dispersive spectroscopy (EDS; Oxford Instruments). The chemical state and composition of NRs surface were probed using X-ray photoelectron spectroscopy (XPS) with Al Kα (1486.6 eV) radiation and the recorded data was calibrated using C-1 s spectrum with the binding energy of 284.6 eV (ESCALAB-MKII spectrometer (UK)).

The gas sensing performance of the flexible ZnO NRs was evaluated at room temperature (~26 °C) under UV-light illumination provided by an UV light-emitting diode (LED, Nichia, λ = 370 nm; 200 μW). The distance between the sensing film and UV-LED was kept at 10 mm. The DC electrical resistance was monitored with a Keithley (model 6514) electrometer under a bias of 1 V. Details about the gas sensing workbench can be found in Ref. [10]. To investigate sensor selectivity, its response was compared with those obtained with other oxidizing and reducing gases, namely CO_2, CO, NO_2, NH_3, and formaldehyde (CH_2O), keeping UV illumination at room temperature. The sensor response (S) was defined as $S = R_{gas}/R_{air}$ for oxidizing gases (O_3, CO_2 and NO_2) and $S = R_{air}/R_{gas}$ for reducing gases (CO, NH_3 and CH_2O), where R_{air} and R_{gas} are the electric resistances of the sensor device exposed to air and target gas, respectively.

Results and discussion

Structural and microstructural characterization

Figure 2(a) shows that as-grown bare ZnO NRs are randomly oriented, with diameter varying between 70 to 300 nm and an average length of 2 μm. Decoration of ZnO surfaces with gold nanoparticles (of ca.10 nm) did not affect the crystal shape of NRs, as seen in Fig. 2(b-c). The XRD patterns of as-prepared pristine ZnO NRs and gold-ZnO NRs are shown in Fig. S2, where all reflections can be indexed to hexagonal wurtzite structure of ZnO (JCPDS file 36–1451). The gold-ZnO sample presented two additional XRD peaks at approximately 38.3° and 44.5°, which can be assigned to metallic gold nanoparticles (JCPDS file 89–3697) [14]. Since the nanorods are randomly oriented, the surface to volume ratio is high, which is expected to enhance the response kinetics towards target gases [15].

The purity of ZnO NRs and gold-ZnO NRs was ensured with the EDS analyses in Fig. S3, where only Zn, O, Au elements were identified uniformly distributed throughout the ZnO NRs. The chemical composition of the surfaces was further confirmed with XPS, whose survey spectra in Fig. S4 indicate the presence of Zn, O and Au elements. The existence of C is attributed to adventitious carbon contamination. The high-resolution spectra of Zn 2p, O 1 s, C 1 s, Au 4d and Au 4f photoelectron lines of ZnO and gold-ZnO NRs are shown in Fig. 3(a-d). The spin–orbit transitions of Zn $2p_{1/2}$ and $2p_{3/2}$ binding energy peaks appear at approximately 1045 and 1021.8 eV, respectively. The binding energy difference between these two lines was 23.2 eV, in good agreement with the reference value of ZnO [16]. The binding energy of O 1 s (Fig. 3(b)) is resolved into two peaks (O_I and O_{II}), one at 528.6 eV assigned to chemisorbed oxygen species (O_2^-) in the Zn–O bonding of the ZnO wurtzite structure and the other at 530.8 eV associated with oxygen deficient regions (O^- and O^{2-} ions) in the sample matrix. The C1s spectrum (Fig. 3(c)) can be deconvoluted into three peaks associated with C–C, C–O, and C = O bands at 284.6 eV, 286.6 eV, and 288.9 eV, respectively. The oxygen and carbon peak matched the reported value [17], with the bands at 82.5 and 86.2 eV in Fig. 3(d) being

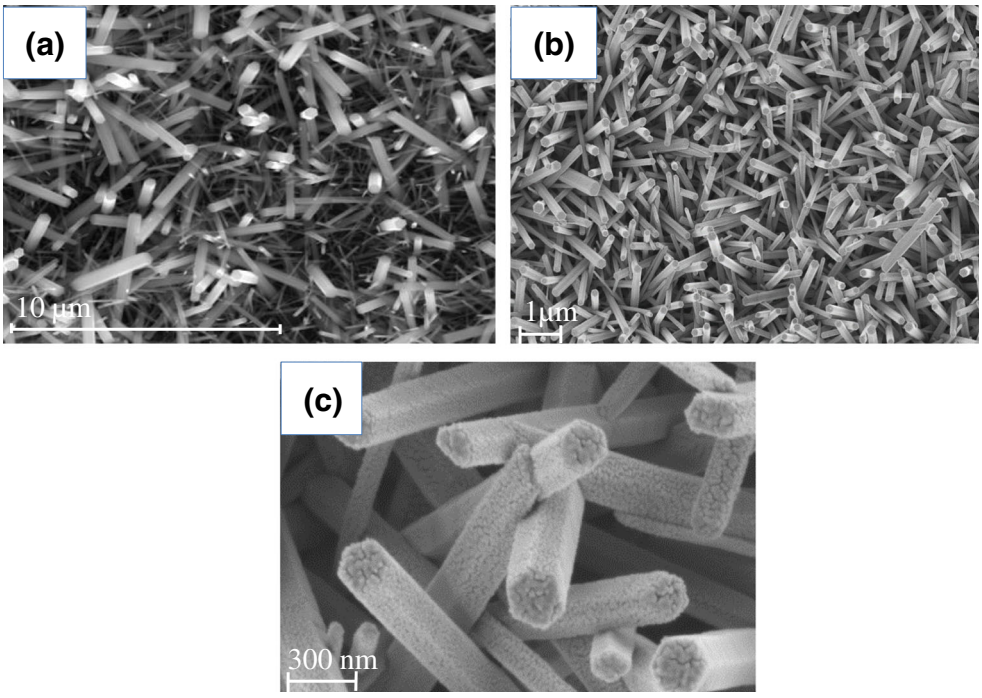

Fig. 2 FESEM images of (**a**) pure ZnO NRs and (**b-c**) low and high magnification gold-ZnO NRs

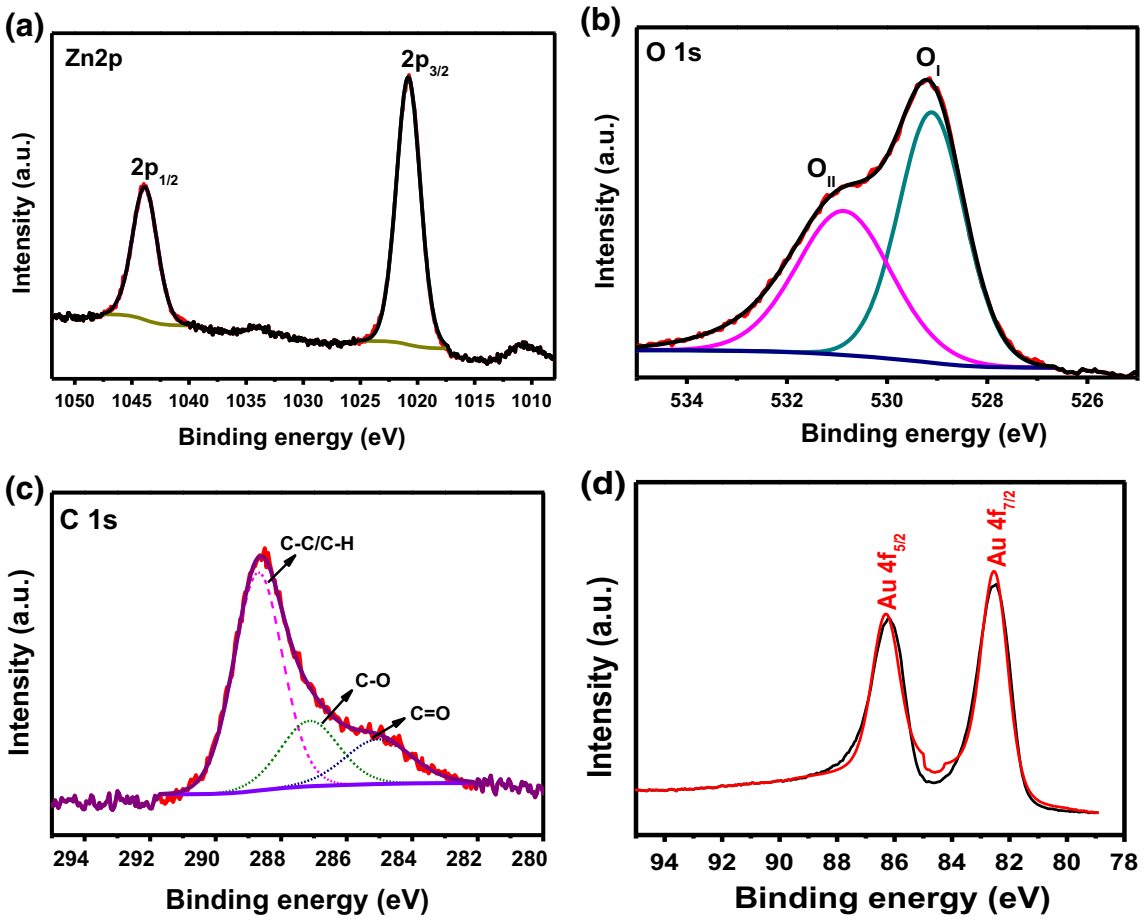

Fig. 3 XPS spectra of (**a**) Zn 2p XPS spectrum; (**b**) O1s XPS spectrum; (**c**) C1s XPS spectrum of pure ZnO NRs, and (**d**) Au 4f for the gold-ZnO NRs

attributed to Au 4f7/2 and Au 4f5/2 [16, 18]. No oxidized gold species are observed, and the peaks at 85.5 and 86.3 eV confirm the presence of metallic gold on the ZnO nanostructures [19].

Gas sensing measurements with ZnO and gold-ZnO nanorods (NRs)

The sensing behavior of pure ZnO NRs in Fig. 4 is typical of n-type semiconductors, since the electrical resistance increases under exposure to an oxidizing gas [20]. The UV illumination did not affect the gas-sensing performance; however, the electrical resistance returned to its initial value when the O_3 exposure was turned off, while no recovery was observed for the sample without UV illumination (in the dark). This latter behavior is due to the slow reaction rate at room temperature, while the UV-LED irradiation provides sufficient energy to release chemisorbed oxygen species attached to ZnO surfaces and induces a fast adsorption-desorption process at room temperature [21, 22].

Sensor performance in terms of sensitivity, selectivity and response time, is normally enhanced by the incorporation of single and binary metal oxides [23, 24], hierarchical metal oxides [25, 26], dopants, conducting polymers [27–29] and surface modification with noble metals such as Pd, Au, Pt [11–13, 30]. Basically, these sensitizers provide additional catalytic sites to enhance surface chemical reactions and electron transfer. Herein, we modified ZnO NRs surface with a ~ 10 nm layer of gold, possibly forming gold clusters which facilitate the transport of charge carriers on the surface of ZnO NRs and improve the overall conductivity of the sensing

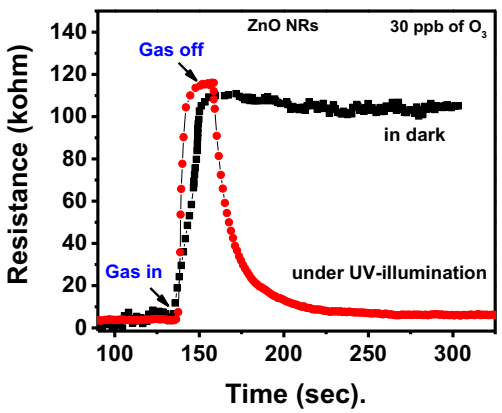

Fig. 4 Resistive response curve of pure ZnO NRs exposed to 30 ppb of O_3 gas under dark and continuous UV irradiation at room temperature

films. The sensitivity and selectivity are expected to increase for the following reasons: (i) a nano-Schottky barrier is formed on the metal oxide surface which should be modulated by the adsorption of gases, thus improving sensitivity, and (ii) the amount of chemisorbed oxygen increases (spillover effect) to create additional active catalytic sites [31–33]. The room temperature response of ZnO and gold-ZnO NRs sensors for concentrations between 30 and 570 ppb of O_3 gas are shown in Fig. 5(a). The response (S) of the gold-ZnO sensor was 108 and 207 for 30 and 570 ppb, respectively, considerably higher than those for the pure ZnO NRs, which was 44 and 76, respectively. The enhancement induced by gold modification can be seen in the enlarged view of the response for 30 ppb of O_3 gas in Fig. 5(b). Furthermore, gold-ZnO NRs exhibited an almost linear dependence of sensor response on ozone exposure up to 570 ppb according to Fig. 5(c). From the data, it is clear that the sensor can detect concentrations below 30 ppb, but in our gas-sensing workbench, it is the lowest concentration that can be reliably exposed to the sensing material. The reliability and reproducibility of the sensor working at room temperature under continuous UV illumination were also evaluated. The results in Fig. 5(d) indicate good repeatability for three testing cycles for 30 ppb O_3 gas.

Figure 6(a) shows the response curve of gold-ZnO NRs at room temperature under UV-illumination, pointing to an improvement in recovery time. The transients for 30 ppb of ozone also revealed a stable response and recovery characteristics. The corresponding response (τ_{res}) and recovery times (τ_{rec}), calculated for 30 ppb ozone, were 13 s and 29 s, respectively. Figure 6(b) shows the selectivity histogram of gold-ZnO NRs films for oxidizing and reducing gases at room temperature under UV-illumination. A negligible response was observed for all the interfering gases, namely CO, CO_2, NO_2, NH_3, and CH_2O. The enhanced performance may be related to electronic sensitization in reaction kinetics which is attributed to the catalytic role of gold in catalytic dissociation of molecular oxygen species [34]. Since the long-term stability and reproducibility of sensing devices is crucial for practical applications, we also tested these features. Fig. S5 shows the long-term stability of a gold-ZnO sensor at room temperature under UV illumination, with the sensor being stable over a period of 12 days, even after repeated exposures to 30 ppb of ozone. The base line resistance and response were found to vary with time due to a "pre-aging" effect typical of most metal oxides from the microstructure of sensing materials operated at low temperatures [35]. Preliminary experiments with bent gold-ZnO sensors indicate that the response/recovery behavior is not significantly affected by bending, as shown in Fig. S6 in the curve for 80 ppb of O_3 under UV-illumination.

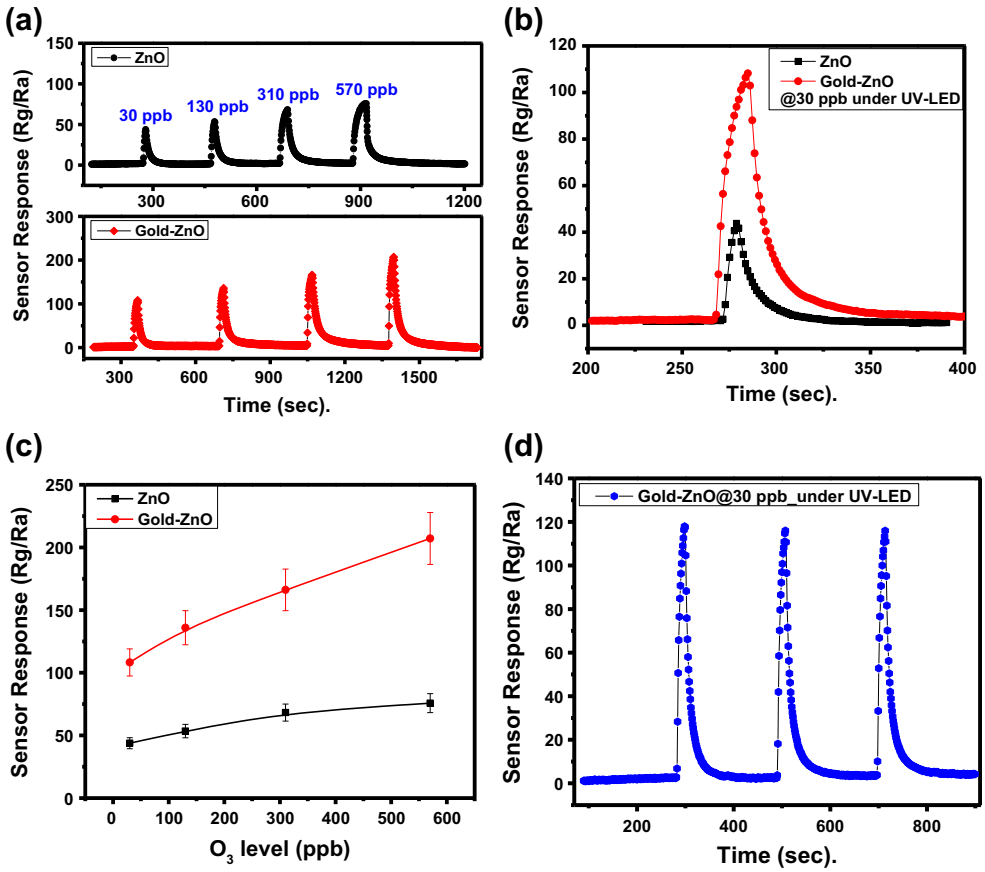

Fig. 5 **a** Room-temperature gas sensing response of ZnO and gold-ZnO for various O_3 gas concentrations under continuous UV-illumination. (**b**) Comparative plot of sensor responses for pure and gold-ZnO NRs exposed to 30 ppb of O_3 gas. (**c**) Variation of sensor response as a function of ozone concentration for pure and gold-ZnO NRs. (**d**) Reproducibility of the three gold-ZnO sensors for 30 ppb of O_3 gas at room temperature with UV illumination

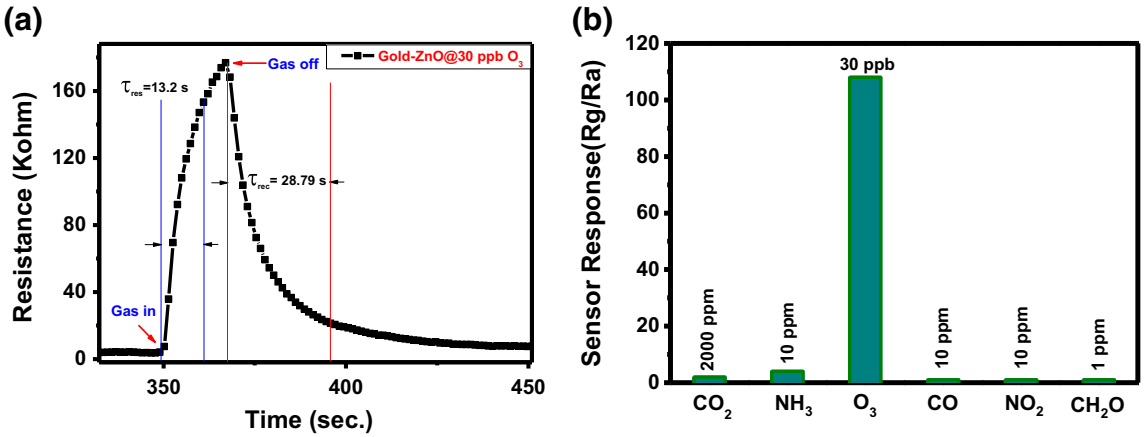

Fig. 6 **a** Typical response-recovery characteristics of gold-ZnO sensor at room temperature for 30 ppb of ozone with UV activation. **b** Selectivity histogram of the gold-ZnO sensor to several possible interferents at room temperature under UV-illumination

Table 1 shows a brief summary of UV-enhanced room temperature ZnO gas sensors compared to our current work. Significantly, the pure and gold-ZnO NRs exhibit enhanced response at room temperature compared to other sensors.

The gas sensing mechanism of metal oxide gas sensors has been proposed in previous reports [10, 11], which may serve to understand the sensing response of gold-ZnO nanorods under UV light illumination. The ozone gas sensing mechanism of gold-ZnO samples under UV light can be explained as follows. At room temperature, the ionic O_2^- species are dominant because oxygen molecules are chemisorbed on ZnO exposed to the air, and electrons are transferred from the conduction band. The ionic species (O_2^-) are formed according to the following reactions [42]:

$$O_2(g) \rightarrow O_2(ads) \quad (1)$$

$$O_2(ads) + e^- \rightarrow O_2^-(ads) \quad (2)$$

A depletion layer is formed on the surface of ZnO NRs as electrons are consumed in the surface region, causing the electrical resistance of ZnO NRs to increase. Under UV light, a large number of electron-hole pairs are generated since the photon energy is higher than the band gap of ZnO. These photo-generated electrons and holes will recombine and many of the photo-generated holes react with oxygen species (O_2^-) on the surface of ZnO NRs in the reaction [20, 43]:

$$h^+(h\nu) + O^{2-}(ads) \rightarrow O_2(g) \quad (3)$$

As a result, oxygen species are photodesorbed from the ZnO surface and the width of the surface depletion layer is reduced. On the other hand, the photo-generated electrons will contribute to the decrease of both the depletion layer width and electrical resistance. Upon exposure, ozone gas adsorbs on the ZnO NRs and photo-generated electrons are released from the surface as they are attracted to the adsorbed ozone molecules to act as electron acceptors (oxidizing gas) [6, 44]:

$$O_3(g) + e^-(h\nu) \rightarrow O_2(des)\ (h\nu) + O^-(ads)\ (h\nu) \quad (4)$$

This reaction broadens the surface depletion layer in ZnO NRs, as depicted schematically in Fig. 7. The electrical resistance is thus increased because the number of electrons participating in the above reaction increases. For gold-ZnO NRs, the ozone gas molecules spilt over ZnO surface, with chemisorption and dissociation of ozone gas enhanced due to the high catalytic activity of gold. In summary, the enhanced

Table 1 UV-enhanced room temperature ZnO-based gas sensors

Sensing Material	Gas Concentration	Operating temperature (°C)	Sensor response (R_g/R_a)	Reference
ZnO	HCHO (100 ppm)	RT	12.61	[36]
gold-ZnO	Ethanol (100 ppm)	RT	1.18	[37]
SnO_2–ZnO	Ozone (20 ppb)	RT	8.0	[6]
CdS/ZnO	NO_2 (1 ppm)	RT	15.3	[38]
In_2O_3	NO (50 ppm)	RT	41.7	[39]
Ag–ZnO	Formaldehyde (40 ppm)	RT	1.2	[40]
Ni-ZnO	Acetone (100 ppm)	RT	1.61	[41]
ZnO	Ozone (30 ppb)	RT	~44	Present Work
gold-ZnO	Ozone (30 ppb)	RT	~108	Present Work

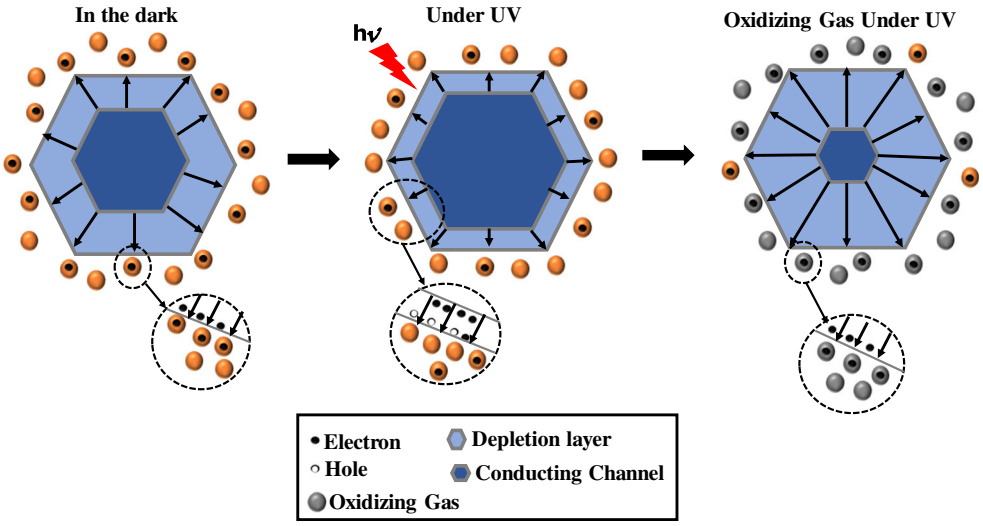

Fig. 7 Schematic illustration of the gas sensing mechanism for the ZnO NRs

sensor response of gold-ZnO is attributed to the increased number of electrons via the transfer process from gold to the conduction band of ZnO, in addition to the strong chemisorption and dissociation of gas molecules. The depletion layer width of ZnO NRs under UV illumination is larger than that in the dark state [45, 46].

Conclusion and further work

ZnO nanorods were successfully deposited on flexible substrates (BOPET) by a simple hydrothermal method to be applied as UV-assisted gas-sensors operating at room temperature. The structural and surface morphology reveals the highly crystalline wurtzite structure with nanorod diameters ranging between 70 to 300 nm with length varying from 1 to 3 μm. ZnO NRs modified with a thin gold layer had good sensing performance for ozone under UV-LED illumination at room temperature. The significant enhancement in the response of the gold-ZnO NRs to ozone gas by UV irradiation was attributed to the photo-generation of electrons and holes. The adsorption of gold enhanced the n-type properties of ZnO as a catalyst to improve gas sensing properties. The flexible gold-ZnO gas sensor may be a suitable candidate for the selective detection of ppb level of ozone gas. In future work, we shall vary the gold thickness to assess its effect on the gas sensing performance and to test the sensor performance for ozone gas at various levels of other parameters such as relative humidity.

Acknowledgements This work had financial support from CNPq and FAPESP (2012/15543-7, 2013/14262-7, 2013/07296-2, 2017/12437-5, 2014/23546-1, 2016 / 23474-6) (Brazil). The authors are also thankful to Berkeley Sensor and Actuator Centre (BSAC). The authors are also grateful to Angelo L. Gobbi and Maria H. O. Piazzetta for the use of the Microfabrication Laboratory (LMF-20509) facilities to manufacture electrodes (LMF/LNNano-LNLS, Campinas, Brazil).

Compliance with ethical standards The author(s) declare that they have no competing interests.

References

1. Zhang J, Liu X, Neri G, Pinna N (2016) Nanostructured materials for room-temperature gas sensors. Adv Mater 28(5):795–831. https://doi.org/10.1002/adma.201503825
2. Joshi N, Hayasaka T, Liu Y, Liu H, Oliveira ON, Lin L (2018) A review on chemiresistive room temperature gas sensors based on metal oxide nanostructures, graphene and 2D transition metal dichalcogenides. Microchim Acta 185(4):213. https://doi.org/10.1007/s00604-018-2750-5
3. Liu D, Lin L, Chen Q, Zhou H, Wu J (2017) Low power consumption gas sensor created from silicon nanowires/TiO2 Core–Shell heterojunctions. ACS Sensors 2(10):1491–1497. https://doi.org/10.1021/acssensors.7b00459
4. Mishra YK, Adelung R (2018) ZnO tetrapod materials for functional applications. Mater Today 21(6):631–651. https://doi.org/10.1016/j.mattod.2017.11.003
5. Chen T-Y, Chen H-I, Hsu C-S, Huang C-C, Wu J-S, Chou P-C, Liu W-C (2015) Characteristics of ZnO nanorods-based ammonia gas sensors with a cross-linked configuration. Sensors Actuators B Chem 221:491–498. https://doi.org/10.1016/j.snb.2015.06.122
6. da Silva LF, M'Peko JC, Catto AC, Bernardini S, Mastelaro VR, Aguir K, Ribeiro C, Longo E (2017) UV-enhanced ozone gas sensing response of ZnO-SnO2 heterojunctions at room temperature. Sensors Actuators B Chem 240:573–579. https://doi.org/10.1016/j.snb.2016.08.158
7. Xu F, H-P HO (2017) Light-activated metal oxide gas sensors: a review. Micromachines 8(11):333
8. Joshi N, Shimizu FM, Awan IT, Peko JM, Mastelaro VR, Oliveira ON, Silva LFd (2016) Ozone sensing properties of nickel phthalocyanine:ZnO nanorod heterostructures. In: 2016 IEEE SENSORS, 30 Oct.-3 Nov. 2016. pp 1–3. https://doi.org/10.1109/ICSENS.2016.7808407
9. Kathiravan D, Huang B-R, Saravanan A (2017) Multifunctional sustainable materials: the role of carbon existing protein in the enhanced gas and UV sensing performances of ZnO-based biofilms. J Mater Chem C 5(21):5239–5247. https://doi.org/10.1039/C7TC01305A

10. Joshi N, da Silva LF, Jadhav HS, Shimizu FM, Suman PH, M'Peko J-C, Orlandi MO, Seo JG, Mastelaro VR, Oliveira ON (2018) Yolk-shelled ZnCo2O4 microspheres: surface properties and gas sensing application. Sensors Actuators B Chem 257:906–915. https://doi.org/10.1016/j.snb.2017.11.041
11. Joshi N, da Silva LF, Jadhav H, M'Peko J-C, Millan Torres BB, Aguir K, Mastelaro VR, Oliveira ON (2016) One-step approach for preparing ozone gas sensors based on hierarchical NiCo2O4 structures. RSC Adv 6(95):92655–92662. https://doi.org/10.1039/C6RA18384K
12. Joshi N, Saxena V, Singh A, Koiry SP, Debnath AK, Chehimi MM, Aswal DK, Gupta SK (2014) Flexible H2S sensor based on gold modified polycarbazole films. Sensors Actuators B Chem 200:227–234. https://doi.org/10.1016/j.snb.2014.04.041
13. Kumar A, Joshi N, Samanta S, Singh A, Debnath AK, Chauhan AK, Roy M, Prasad R, Roy K, Chehimi MM, Aswal DK, Gupta SK (2015) Room temperature detection of H2S by flexible gold–cobalt phthalocyanine heterojunction thin films. Sensors Actuators B Chem 206:653–662. https://doi.org/10.1016/j.snb.2014.09.074
14. Guo J, Zhang J, Zhu M, Ju D, Xu H, Cao B (2014) High-performance gas sensor based on ZnO nanowires functionalized by au nanoparticles. Sensors Actuators B Chem 199:339–345. https://doi.org/10.1016/j.snb.2014.04.010
15. Ramgir NS, Kaur M, Sharma PK, Datta N, Kailasaganapathi S, Bhattacharya S, Debnath AK, Aswal DK, Gupta SK (2013) Ethanol sensing properties of pure and au modified ZnO nanowires. Sensors Actuators B Chem 187:313–318. https://doi.org/10.1016/j.snb.2012.11.079
16. Hosseini ZS, Mortezaali A, Iraji zad A, Fardindoost S (2015) Sensitive and selective room temperature H2S gas sensor based on au sensitized vertical ZnO nanorods with flower-like structures. J Alloys Compd 628:222–229. https://doi.org/10.1016/j.jallcom.2014.12.163
17. Liu W, Tang X, Tang Z, Chu F, Zeng T, Tang N (2014) Role of oxygen defects in magnetic property of cu doped ZnO. J Alloys Compd 615:740–744. https://doi.org/10.1016/j.jallcom.2014.07.033
18. Mohapatra S, Mishra YK, Avasthi DK, Kabiraj D, Ghatak J, Varma S (2008) Synthesis of gold-silicon core-shell nanoparticles with tunable localized surface plasmon resonance. Appl Phys Lett 92(10):103105. https://doi.org/10.1063/1.2894187
19. Wang A-Q, Liu J-H, Lin SD, Lin T-S, Mou C-Y (2005) A novel efficient au–ag alloy catalyst system: preparation, activity, and characterization. J Catal 233(1):186–197. https://doi.org/10.1016/j.jcat.2005.04.028
20. Catto AC, da Silva LF, Ribeiro C, Bernardini S, Aguir K, Longo E, Mastelaro VR (2015) An easy method of preparing ozone gas sensors based on ZnO nanorods. RSC Adv 5(25):19528–19533. https://doi.org/10.1039/C5RA00581G
21. Dhahri R, Hjiri M, Mir LE, Bonavita A, Iannazzo D, Latino M, Donato N, Leonardi SG, Neri G (2016) Gas sensing properties of Al-doped ZnO for UV-activated CO detection. J Phys D Appl Phys 49(13):135502
22. Yayu Z, Xuan L, Ping D, Yuxin N, Yan Z, Lili X, Xinyu X (2014) Pt/ZnO nanoarray nanogenerator as self-powered active gas sensor with linear ethanol sensing at room temperature. Nanotechnology 25(11):115502
23. Lee J-H (2009) Gas sensors using hierarchical and hollow oxide nanostructures: overview. Sensors Actuators B Chem 140(1):319–336. https://doi.org/10.1016/j.snb.2009.04.026
24. Woo H-S, Na CW, Lee J-H (2016) Design of Highly Selective gas Sensors via physicochemical modification of oxide nanowires: overview. Sensors (Basel, Switzerland) 16(9):1531. https://doi.org/10.3390/s16091531
25. Gao Y, Kong Q, Zhang J, Xi G (2017) General fabrication and enhanced VOC gas-sensing properties of hierarchically porous metal oxides. RSC Adv 7(57):35897–35904. https://doi.org/10.1039/C7RA06808E
26. Li Y-X, Guo Z, Su Y, Jin X-B, Tang X-H, Huang J-R, Huang X-J, Li M-Q, Liu J-H (2017) Hierarchical morphology-dependent gas-sensing performances of three-dimensional SnO2 nanostructures. ACS Sensors 2(1):102–110. https://doi.org/10.1021/acssensors.6b00597
27. Mekki A, Joshi N, Singh A, Salmi Z, Jha P, Decorse P, Lau-Truong S, Mahmoud R, Chehimi MM, Aswal DK, Gupta SK (2014) H2S sensing using in situ photo-polymerized polyaniline–silver nanocomposite films on flexible substrates. Org Electron 15(1):71–81. https://doi.org/10.1016/j.orgel.2013.10.012
28. Singh A, Salmi Z, Joshi N, Jha P, Kumar A, Lecoq H, Lau S, Chehimi MM, Aswal DK, Gupta SK (2013) Photo-induced synthesis of polypyrrole-silver nanocomposite films on N-(3-trimethoxysilylpropyl)pyrrole-modified biaxially oriented polyethylene terephthalate flexible substrates. RSC Adv 3(16):5506–5523. https://doi.org/10.1039/C3RA22981E
29. Ghoorchian A, Alizadeh N (2018) Chemiresistor gas sensor based on sulfonated dye-doped modified conducting polypyrrole film for high sensitive detection of 2,4,6-trinitrotoluene in air. Sensors Actuators B Chem 255:826–835. https://doi.org/10.1016/j.snb.2017.08.093
30. Ponzoni A, Baratto C, Cattabiani N, Falasconi M, Galstyan V, Nunez-Carmona E, Rigoni F, Sberveglieri V, Zambotti G, Zappa D (2017) Metal oxide gas sensors, a survey of selectivity issues addressed at the SENSOR lab, Brescia (Italy). Sensors (Basel, Switzerland) 17(4):714. https://doi.org/10.3390/s17040714
31. Liu C, Kuang Q, Xie Z, Zheng L (2015) The effect of noble metal (au, Pd and Pt) nanoparticles on the gas sensing performance of SnO2-based sensors: a case study on the {221} high-index faceted SnO2 octahedra. CrystEngComm 17(33):6308–6313. https://doi.org/10.1039/C5CE01162K
32. Rai P, Majhi SM, Yu Y-T, Lee J-H (2015) Noble metal@metal oxide semiconductor core@shell nano-architectures as a new platform for gas sensor applications. RSC Adv 5(93):76229–76248. https://doi.org/10.1039/C5RA14322E
33. Ramgir NS, Sharma PK, Datta N, Kaur M, Debnath AK, Aswal DK, Gupta SK (2013) Room temperature H2S sensor based on au modified ZnO nanowires. Sensors Actuators B Chem 186:718–726. https://doi.org/10.1016/j.snb.2013.06.070
34. Basu S, Basu PK (2009) Nanocrystalline metal oxides for methane sensors: role of Noble metals. Journal of Sensors 2009:1–20. https://doi.org/10.1155/2009/861968
35. Korotcenkov G (2007) Metal oxides for solid-state gas sensors: what determines our choice? Mater Sci Eng B 139(1):1–23. https://doi.org/10.1016/j.mseb.2007.01.044
36. Cui J, Shi L, Xie T, Wang D, Lin Y (2016) UV-light illumination room temperature HCHO gas-sensing mechanism of ZnO with different nanostructures. Sensors Actuators B Chem 227:220–226. https://doi.org/10.1016/j.snb.2015.12.010
37. Wongrat E, Chanlek N, Chueaiarrom C, Samransuksamer B, Hongsith N, Choopun S (2016) Low temperature ethanol response enhancement of ZnO nanostructures sensor decorated with gold nanoparticles exposed to UV illumination. Sensors Actuators A Phys 251:188–197. https://doi.org/10.1016/j.sna.2016.10.022
38. Geng X, Zhang C, Debliquy M (2016) Cadmium sulfide activated zinc oxide coatings deposited by liquid plasma spray for room temperature nitrogen dioxide detection under visible light illumination. Ceram Int 42(4):4845–4852. https://doi.org/10.1016/j.ceramint.2015.11.170
39. Chinh ND, Quang ND, Lee H, Thi Hien T, Hieu NM, Kim D, Kim C, Kim D (2016) NO gas sensing kinetics at room temperature under UV light irradiation of In2O3 nanostructures. Sci Rep 6:35066. https://doi.org/10.1038/srep35066 https://www.nature.com/articles/srep35066#supplementary-information

40. Cui J, Wang D, Xie T, Lin Y (2013) Study on photoelectric gas-sensing property and photogenerated carrier behavior of Ag–ZnO at the room temperature. Sensors Actuators B Chem 186:165–171. https://doi.org/10.1016/j.snb.2013.05.088
41. Ahn H, Wang Y, Hyun Jee S, Park M, Yoon YS, Kim D-J (2011) Enhanced UV activation of electrochemically doped Ni in ZnO nanorods for room temperature acetone sensing. Chem Phys Lett 511(4):331–335. https://doi.org/10.1016/j.cplett.2011.06.045
42. Barsan N, Koziej D, Weimar U (2007) Metal oxide-based gas sensor research: how to? Sensors Actuators B Chem 121(1):18–35. https://doi.org/10.1016/j.snb.2006.09.047
43. Cao C, Hu C, Wang X, Wang S, Tian Y, Zhang H (2011) UV sensor based on TiO2 nanorod arrays on FTO thin film. Sensors Actuators B Chem 156(1):114–119. https://doi.org/10.1016/j.snb.2011.03.080
44. Fan S-W, Srivastava AK, Dravid VP (2009) UV-activated room-temperature gas sensing mechanism of polycrystalline ZnO. Appl Phys Lett 95(14):142106. https://doi.org/10.1063/1.3243458
45. Li X, Zhang Y, Ren X (2009) Effects of localized surface plasmons on the photoluminescence properties of au-coated ZnO films. Opt Express 17(11):8735–8740. https://doi.org/10.1364/OE.17.008735
46. Xuming Z, Yu Lim C, Ru-Shi L, Din Ping T (2013) Plasmonic photocatalysis. Rep Prog Phys 76(4):046401. https://doi.org/10.1088/0034-4885/76/4/046401